Theoretical and experimental investigations of subpicosecond photoconductivity

S. N. Chamoun, R. Joshi, E. N. Arnold, and R. O. Grondin
Center for Solid State Electronics Research, Arizona State University, Tempe, Arizona 85287

K. E. Meyer
Cavendish Laboratory, University of Cambridge, Cambridge, United Kingdom

M. Pessot
Laboratory for Laser Energetics, University of Rochester, Rochester, New York 14627

G. A. Mourou
Department of Electrical Engineering and Computer Science, University of Michigan, Ann Arbor, Michigan 48109-1120

(Received 9 February 1989; accepted for publication 16 March 1989)

Monte Carlo methods are used to study photoconductive transients in gallium arsenide. It is demonstrated that working with presently established ranges for the Γ-L coupling coefficient, the existence of a velocity overshoot at moderate fields cannot be exactly predicted. The role of negative velocity electrons in the initial transient for short wavelength excitation is also demonstrated. Details of an actual experiment are described and evaluated against a model which incorporates the Monte Carlo simulation into a transmission line structure with a frequency-dependent characteristic impedance. The results demonstrate that an appropriately designed experiment can observe subpicosecond carrier transport transients.

I. INTRODUCTION

After some 20 years of investigation, the field of transient hot carrier transport remains a field in which there are too few experiments. Recently, photoconductive transients have been produced and suggested as a basis for the experimental study of transport transients.[1–7] In this paper we consider the physical basis for such experiments, describe one actual experiment, and discuss the future potential for such studies.

The material system which we will consider is gallium arsenide. Electron transport transients in GaAs generally are dominated by either a net transfer of electrons from the Γ conduction-band valley to the L and X valleys, or alternatively by a net transfer from the higher-energy valleys back to the Γ valley. The most commonly discussed transient, the velocity overshoot first predicted by Ruch,[8] starts with electrons in the Γ valley in an equilibrium state. On the sudden application of a electric field, these electrons are accelerated to high velocity states in the Γ valley and then scatter to lower velocity states in the L or X valleys. A typical Monte Carlo calculation of this type of transient is shown in Fig. 1. The conduction-band parameters of Table I were used and the details of the scattering mechanisms included have been discussed by Osman and Ferry.[9] The second behavior in which electrons must transfer from the L valley back to the Γ valley, while less commonly mentioned, was actually the first to be simulated. In 1969 Rees[10] used an iterative solution to the Boltzmann equation to produce transients similar to the Monte Carlo transients shown in Fig. 2. Here an initial electric field of 6 kV/cm has been applied for a long time and the electrons have settled into the corresponding steady-state distribution. The field is then suddenly stepped down to the level indicated by the parameters of the curves in Fig. 2. As can be seen, the velocity rapidly drops and then rises to the appropriate final steady-state value. In some instances, this depressed velocity could have a detrimental effect on device performance (e.g., Ref. 11). Its physical origin, however, is well known and when seen in Gunn device simulations is sometimes referred to as the Jones–Rees effect.[12] This is illustrated in Fig. 3. When carriers enter the Γ valley from the L valley they can take on either a positive or a negative velocity. It is the presence of the field, however, that establishes a difference between positive and negative velocity carriers. Electrons entering with a positive velocity gain energy from the field and therefore are ballistically placed into states above the intervalley scattering threshold. Electrons entering the Γ valley with a negative velocity, however, lose energy to the field and are ballistically placed into states

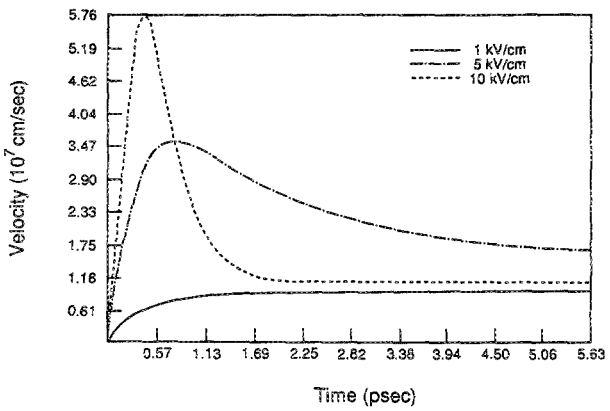

FIG. 1. Transient electron velocity for applied fields of 1, 5, 10 kV/cm assuming an initial Maxwellian distribution.

 0021-8979/89/130236-11$02.40

TABLE I. Parameters of GaAs Monte Carlo program.

Parameter		Γ	L	X
Density (g/cm^3)	5.37			
Energy-band gap at 300 K (eV)	1.43			
High-frequency dielectric constant	10.92			
Static dielectric constant	12.9			
Velocity of sound (cm/s)	5.22×10^5			
Number of valleys		1	4	3
Effective mass ratio		0.063	0.222	0.58
Nonparabolicity factor (eV^{-1})		0.61	0.46	0.20
Valley separation from Γ valley (eV)			0.29	0.49
Polar optic-phonon energy (eV)		0.0364	0.0364	0.0364
Acoustic deformation potential (eV)		7.0	7.0	7.0
Coupling constant (10^8 eV/cm)	Γ to		7	10
	L to	7	10	5
	X to	10	5	10
Intervalley phonon energy (eV)	0.0311			
Heavy-hole band	0.45			
Light-hole band	0.082			
Split-off band	0.17			

below the intervalley scattering threshold. The result is that the transfer from L to Γ valley predominantly uses the negative velocity states, thus producing the transient dip seen in Fig. 2. As noted by Jones and Rees,[13] such a transfer during the accumulation transit mode of Gunn devices gives rise to a carrier cooling effect by aiding the transfer out of the higher energy valley and may augment Gunn device performance.

Although there have been attempts at extracting information concerning these transients from dc I-V curves, success to date has relied on building either extremely short gate field-effect transistors (FETs)[14] or special purpose structures.[15,16] While these experiments do strongly indicate that these transient transport effects are present, they necessarily involve both spatial and temporal averaging. Here we will consider the other main strategy, which is to attempt to temporally resolve the behaviors of interest. The strategy which would seem to be indicated by the theoretical studies, that of stepping the voltage applied across a semiconductor sample and then measuring the terminal current, has several obvious disadvantages. First, it is extremely difficult to make the voltage applied to a semiconductor sample perform one of these steps. Second, even if it were possible there would be a large capacitive contribution (associated with this time-varying voltage) to the measured terminal current. This capacitive contribution would complicate the analytical process by which a time-varying conduction current is extracted from the measured terminal current. In view of these difficulties, a better alternative is to perform experiments which rely on using very short optical pulses to suddenly generate electron-hole pairs in an already extant electric field.

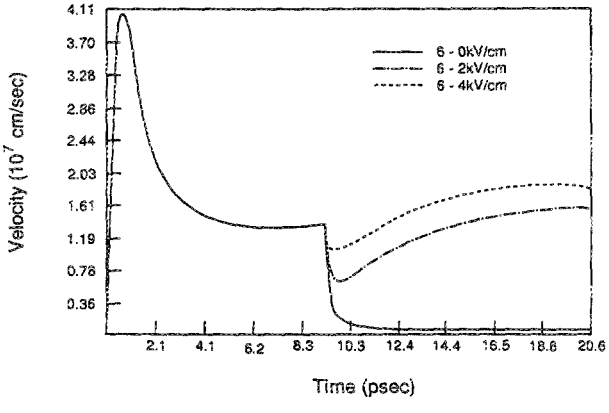

FIG. 2. Transient electron velocity response to fields stepped from 6 kV/cm down to 0, 2, and 4 kV/cm. The initial electrons distribution is taken to be Maxwellian.

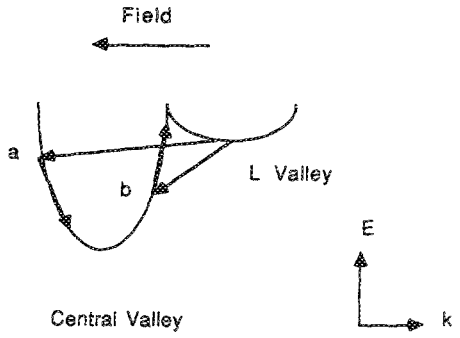

FIG. 3. Schematic diagram of the Jones–Rees effect. The return of the electrons from the L valley involves two possible outcomes, one where (a) electrons lose energy and remain in the central valley, and (b) the other where electrons gain energy and transfer back to the L valley.

II. TIME DOMAIN AND FREQUENCY DOMAIN EXPERIMENTS

The optical experiments remove the first of the difficulties mentioned above by allowing us to rapidly place the system into an initial state. The challenge in an optical experiment is the measurement of the transient photoresponse in which the system moves from this initial state into a final state. Many commonly used spectral techniques do not provide information on the average momentum of the carriers. Yet it is the momentum that needs to be measured in any experimental study of a velocity overshootlike behavior. Several "probes" have been used in efforts to determine conduction currents and momentum behaviors. Time-resolved terminal current measurements,[1,2] time-resolved reflectivity measurements,[3] and time-resolved absorption measurements[17] have all been used. In all cases the response (in the presence of an applied bias) is determined by the mechanisms in which current continuity is maintained during the

transient. Therefore, we start our discussion by reviewing transient current continuity.

A bias-dependent field component is needed in a velocity overshoot study. Therefore, terminals are needed even if the terminal current is not observed. At these terminals there will be a "surface" charge that steps the field down from the value it has inside the semiconductor to the nearly zero value that it has inside the external circuit. When electron-hole pairs are generated in this applied field they separate and move in opposite directions. As they do so, a time-varying contribution to the field arises from the space-charge movement. Locally, inside the sample, there is a displacement current associated with this field variation. This local displacement current is essential for current continuity. While there is a particle current only in regions where there are moving particles, the field, which evolves everywhere inside the sample, creates a spatially dependent, time-varying displacement current. The time-varying field at the terminals induces the terminal surface charge to vary in time. Therefore, a current must flow in the bias circuit. This is the induced current of Ramo[18] and Shockley[19] upon which microwave time-of-flight measurements of carrier drift velocities[20,21] are based. As this current flows in the external circuit there will be a change in the voltage applied across the sample. This time-varying voltage also creates a displacement current contribution at all points inside the sample and a capacitive contribution to the current flowing at the terminals. Therefore, there are two sources of displacement current flow inside the sample. The space-charge contribution is needed but the capacitive contribution is an undesirable parasitic.

The first transient optical experiment was that of Shank *et al.*[17] in 1981. They performed a pump-probe experiment in which carriers were photogenerated in GaAs with an 805-nm wavelength pulse, and a second pulse was absorption measurement as a probe of the time-varying field inside the sample. An electric field alters the band-edge optical absorption by the Franz–Keldysh effect[22] and Shank *et al.* were able to do a time-resolved measurement of this absorption edge shift. They ignored any capacitive contributions to the field variation and were able to use the concepts discussed above to relate the time-varying field to carrier movement in space. In their analysis they used a constant hole velocity and a time-varying electron velocity. They found it was necessary to assume that the electron velocity during the first picosecond or so of the transient was about three times larger than the final steady-state velocity.

A second all-optical technique was developed by Nuss, Auston, and Capasso.[3] In their experiment there was no bias voltage applied to the sample. They used the time-varying field associated with an optical pulse itself to accelerate the photogenerated carriers. Their experiment therefore does not closely resemble the normal velocity overshoot conditions. They photogenerated carriers with a pump pulse of 625 nm and then measured with subpicosecond resolution a time-resolved optical reflectivity of the system. From this data they extracted a time-varying mobility which exhibited no overshoot but took several picoseconds to rise to a final value. Since there is no electric field imposed the lack of an overshoot is not troublesome. The slow rise in mobility was the significant result. Nuss *et al.* hypothesized that as they were photogenerating carriers high in the Γ valley, above the Γ-L transfer threshold, the carriers were transferring to the L valley very rapidly after the photogeneration. The mobility, therefore, started low and then slowly rose as the carriers returned to the Γ valley. Osman and Grubin[4] have performed a Monte Carlo study in which photogeneration by the same wavelength in a relatively low electric field (500 V/cm) was simulated. They saw exactly the sort of valley transfer behavior hypothesized by Nuss *et al.*

A similar behavior is present in high excitation photoluminescence experiments. There a hot plasma is generated in an unbiased sample and time-resolved luminescence is used to watch the system relax. The relaxation occurs relatively slowly. Two competing theories for this have been proposed. In one, the hot carriers are hypothesized to emit optical phonons sufficiently rapidly creating an increase in the phonon population. Subsequently, the hot carriers reabsorb the phonons that they have emitted, thereby increasing the phonon absorption rate and slowing the energy relaxation.[23] The second explanation is essentially the same as the intervalley transfer picture of Nuss *et al.* Shah *et al.*[24] have performed a comparison between experimental studies of this sort and Monte Carlo calculations. They found that the intervalley scenario did explain the data well but that care had to be taken in the selection of the Γ-L coupling coefficient, a parameter which is generally used as an adjustable parameter in Monte Carlo studies (due to the lack of either direct experimental information or any acceptable computation of this parameter from more basic ones).

The main technique of interest here is the use of time-resolved terminal measurements of the conductivity of carriers photogenerated into an already extant field. Early variations on this have been reported by Hammond[1] and by Mourou *et al.*[2] In both experiments a gap was left in a transmission line on top of a semi-insulating GaAs substrate. A pump pulse was focused on the gap and as the photocurrent in the gap evolved, a time-varying voltage wave was transmitted down the transmission line. The analysis of Auston[25] was used in both experiments to explain why a photoconductive overshoot should produce a transmission line overshoot. The two experiments both used 620-nm wavelength pumps and differed primarily in the temporal resolution of the measurement of the voltage wave. Hammond used an ion-bombarded second gap as a high-speed photoconductive sampler while Mourou *et al.* abutted an electro-optic sampling crystal against their sample, extended the transmission line onto this sampling crystal, and used a second pulse to electro-optically sample[26] the voltage wave. The temporal resolution of Hammond was about 6 ps, which complicated his interpretation. However, his results were consistent with the general idea of having no overshoot at very low fields, a temporally extended overshoot (lasting several picoseconds) at medium fields, and a temporally sharp overshoot at high fields. Mourou *et al.* had temporal resolution of about 0.5 ps and clearly saw an overshoot very similar to that of Fig. 1.

There are important complications in analyzing both of these experiments. First, in the experiment of Mourou *et al.*,

there is an impedance mismatch between the photoconductive gap and the sampler. The second is that it is unlikely that good ohmic contacts and uniform fields were attained in either system. A third problem is that the subject of transient carrier transport in semi-insulating GaAs has not been extensively studied. Lastly, the potential role of trapping in semi-insulating GaAs is present in both experiments. In short, while it is clear that a photoconductive overshoot occurred, it cannot be unambiguously associated with a velocity overshoot.

It of course is possible to use frequency domain methods as well. Teitai and Wilkins[27] have argued that the existence of a velocity overshoot is implied by a peak in the small-signal ac conductivity. Allen *et al.*[28] have used optical transmission studies to measure the ac conductivity from low frequencies out to 1200 GHz. Their sample was a grid structure laid down on GaAs doped at 10^{17} cm^{-3}. They saw a peak in the conductivity but unfortunately it is virtually certain that the fields present in their system were not spatially uniform as a result of space-charge domain structures.

III. MONTE CARLO STUDIES

The simplest approach to understanding the potential for using such experiments as that of Hammond or Mourou *et al.* for studying transient carrier transport is to perform a Monte Carlo study. A set of valence band parameters is used and carriers are photogenerated out of these bands into the conduction bands by photons of a specified wavelength. A spatially uniform field is assumed and one then studies the transient response of the photogenerated electrons in this field. Several results of this sort have already been reported,[2,4–7] but to date no parameter sensitivity study has been carried out. Additionally, the details of how overshoot can occur for short wavelength photoexcitation have not been clearly described. Lastly, there is a bias-dependent delay seen in the initial rise of the velocity following short wavelength photoexcitation that has not been described in detail. All three tasks will be performed here.

We first conduct a survey of the parameters used for the ensemble Monte Carlo simulation. Four different sets of parameters will be used to examine the sensitivity of transient electron velocity curves. Special attention will be given to the Γ-L deformation potential and its effect on the velocity overshoot phenomena. The purpose of the parameter survey is twofold. First, it yields some quantitative bounds on the accuracy of theoretical simulations. Second, it is indicative of the critical parameters. The Monte Carlo program used for the simulation includes carrier photogeneration out of the heavy-hole, light-hole, and split-off bands. The optical transitions are calculated using the small wave-vector approximations for the wave functions described by Kane.[29] Higher order effects such as damping and lifetime broadening are not included. All the relevant carrier-phonon scattering processes were taken into account. These include the deformation potential and the polar coupling to both the acoustic and optical modes. Carrier-carrier scattering is not included since it is not of importance at laser excitation intensities below 5×10^{17} cm^{-3}.[30] For high density cases, both carrier-carrier and degeneracy effects would have to be included. Furthermore, hot phonon effects are also not considered because no hot phonon buildup can occur at the femtosecond time scale and low photon density that is of interest here.[31] Earlier work[5] has clearly shown a wavelength threshold. The threshold wavelength is the wavelength at which carriers begin to be photogenerated into states above the energy threshold for intervalley scattering. For long wavelengths the system exhibits a Ruch-like velocity overshoot behavior. For short wavelengths new features appear in the transient response, and here we will focus our attention on this short wavelength case.

The transient electron velocity for electric fields values of 1, 3, 5, and 10 kV/cm and laser pulse wavelength of 620 nm using four different parameter sets [given in Table I (Refs. 9 and 24)] are shown in Figs. 4–7. These sets contain combinations of experimentally obtained and theoretically evaluated values. The need for including some theoretical values arises because not all the data have been experimentally measured, but rather inferred indirectly or extrapolated[32] in some manner. In Fig. 4 there is a noticeable velocity overshoot which lasts for about 0.5 ps. for the electric field value of 10 kV/cm. Figure 5 shows the transient velocity curves using the set of parameters used by Wysin, Smith, and Redondo.[7] Their deformation potential parameters are identical with those of Brennan and Hess,[33] while their effective masses were based on a pseudopotential calculation. For electric field values of 1, 3, and 5 kV/cm, the two graphs are in excellent agreement. However, for an electric field of 10 kV/cm, the velocity increases to a steady-state value and no overshoot is observed.

A third parameter set, given by Taylor, Erskine, and Tang[34] is also used to compute the transient velocity which is shown in Fig. 6. The main difference between this set and the set in Table I is in the valence-band parameters. The fourth set of parameters is that of Shah *et al.*[24] and the results obtained using these parameters are presented in Fig. 7. By comparing the four sets of figures, we can conclude that all them are in good agreement with the variation in the peak

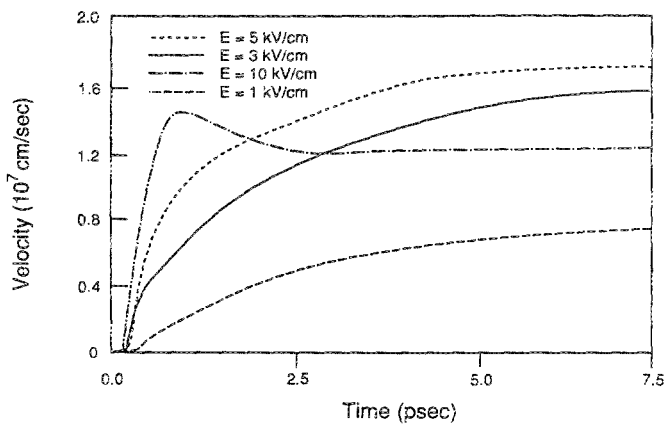

FIG. 4. Transient electron velocity for GaAs obtained by Monte Carlo calculations using the parameter set shown in Table I. The applied fields were 1, 3, 5, and 10 kV/cm, and the electrons were photoexcited using a laser pulse of energy 2.0 eV and width of 100 fs (FWHM).

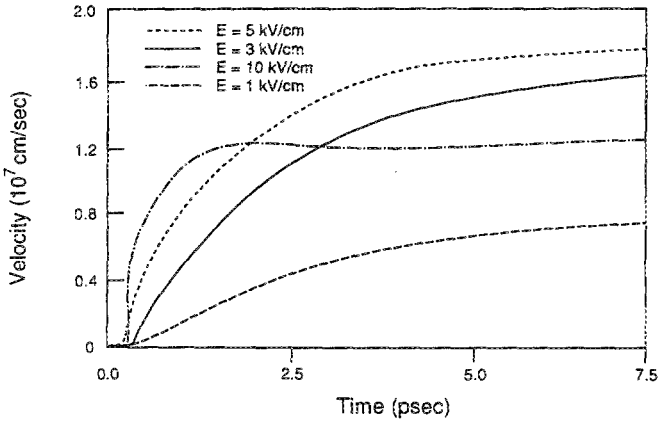

FIG. 5. Transient electron velocity obtained using the parameter set in Table II for fields of 1, 3, 5, and 10 kV/cm. The laser pulse energy is 2.0 eV and its width is 100 fs (FWHM).

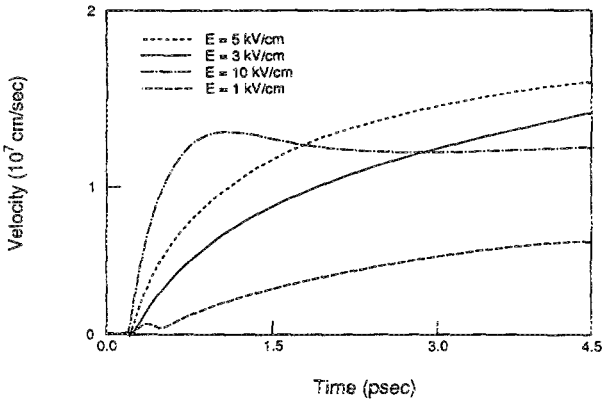

FIG. 7. Transient electron velocity for the parameters given by Shah *et al.* (Ref. 24) for 1, 3, 5, and 10 kV/cm and the same laser pulse used before.

velocity being less than 20%. However, there is a potentially measurable difference in the value of the minimum field at which a velocity overshoot is predicted for a given excitation wavelength.

Velocity overshoots and other transient phenomena are sensitive to the Γ to L deformation potential ($D_{\Gamma L}$) of the conduction band. We have investigated the role of $D_{\Gamma L}$ in influencing the velocity overshoot phenomena at $E = 10$ kV/cm for 2-eV photoexcitation. For concreteness we shall use the recent experimental data of Shah *et al.* who have already performed a subpicosecond luminescence experiment to determine the intervalley deformation potential ($D_{\Gamma L}$) in GaAs. In that experiment, GaAs and InP samples were excited by a subpicosecond pulse and the luminescence intensity was measured. The luminescence intensity for GaAs increased very slowly in contrast with that of InP. Since there is no significant intervalley scattering in InP at the excitation energy used, the slow rise in luminescence in GaAs was attributed to the return of the L-valley electrons to the Γ valley. Their experimental results were compared with an ensemble Monte Carlo calculation and the Γ-L deformation potential was determined to be $(6.5 \pm 1.5) \times 10^8$ eV/cm.

The uncertainty in the experimentally determined value of $D_{\Gamma L}$ translates into rather large deviation of the transient velocities, as we shall now show. Keeping within the error range of Shah *et al.*,[24] we repeated a computation of the transient electron velocity for carriers photogenerated with a wavelength of $\lambda = 620$ nm into a field of 10 kV/cm. Three Γ-L deformation potential values (5×10^8, 6.5×10^8, and 8×10^8 eV/cm) were used. The results are shown in Fig. 8. The velocity curve for $D_{\Gamma L} = 5\times10^8$ eV/cm shows a significant overshoot compared to the other two values of $D_{\Gamma L}$. The velocity curve for $D_{\Gamma L} = 6.5\times10^{18}$ eV/cm shows a slight peak while that for $D_{\Gamma L} = 8\times10^8$ eV/cm just increases to a steady-state velocity. It therefore seems that the existence of an overshoot at $E = 10$ kV/cm for 2.0-eV excitation can only be determined experimentally. Such an experiment would help determine the $D_{\Gamma L}$ value. Since it would look at the departure of the electrons from Γ valley to L valley, it would complement the experiment of Shah *et al.*[24] which observed the L-to-Γ transition.

Even when there is a velocity overshoot following a short wavelength photoexcitation, it differs in detail from

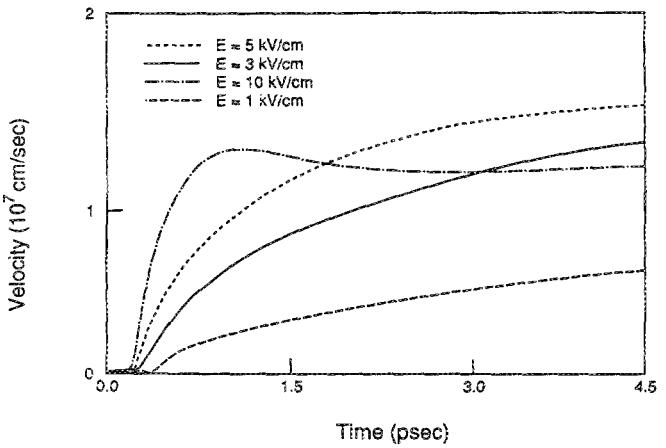

FIG. 6. Transient electron velocity using the parameters given by Taylor *et al.* (Ref. 34) for fields of 1, 3, 5, and 10 kV/cm. The laser pulse specifications are the same as for Fig 5.

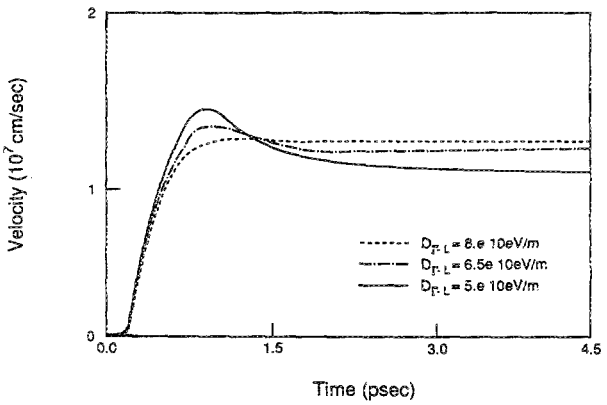

FIG. 8. Transient electron velocity for Γ-L deformation values of 5, 6.5, and 8×10^{10} eV/m as given in Shah *et al.* (Ref. 24). The applied field is 10 kV/cm, and the laser pulse energy is 2.0 eV.

that of the conventional Ruchlike-overshoot. When a short wavelength laser pulse (i.e., $\lambda = 620$ nm) excites a GaAs sample, electrons are photogenerated high in the central valley above the threshold energy for intervalley scattering. These electrons have no net momentum initially. Under the influence of a high electric field (i.e., greater or equal to 20 kV/cm), electrons with initial negative velocity will either be ballistically accelerated to states below the threshold energy for intervalley scattering, E_{int}, or scatter to one of the satellite valleys. The electrons that fall below E_{int} are trapped in the central valley and keep losing energy to the field as long as they have negative velocities.[5]

Examining the drift velocity curves for 2.0-eV excitation (Fig. 4), we note a shift in the initial rise of the velocity that depends on the value of the electric field. In order to explain this phenomena, the electrons photogenerated were classified into six groups as shown in Fig. 9. Groups 1, 2, and 3 are electrons photogenerated from the heavy-hole, light-hole, and split-off bands, respectively, with an initial negative velocity; groups 4, 5, and 6 electrons come from the same valence bands but with an initial positive velocity. The time evolution of the fraction of each of these groups of electrons in the Γ valley is shown in Figs. 10 and 11 for $E = 20$ kV/cm, excitation energy of 2.0 eV, and pulse width (FWHM) of 20 fs.

Since group 1 electrons are generated high in the band, they will either transfer to the satellite valley or lose energy to the field and fall below E_{int}. Thus, their fraction will undershoot and then increase to steady-state value. The fraction of group 4 electrons will undergo a similar behavior to that of group 1 but the population undershoot is more pronounced because these electrons possess positive momentum initially and the majority rapidly leave the central valley.

The fractional populations of groups 2 and 3 both overshoot their steady-state value because they are trapped in the Γ valley below E_{int}. On the other hand, the corresponding positive velocity groups 5 and 6 start low in the Γ valley and will stay there until they gain enough energy from the field to transfer to the satellite valleys. Therefore, their fractions will

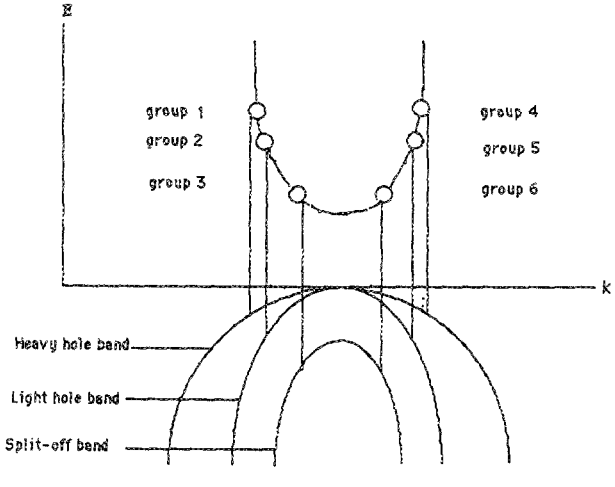

FIG. 9. Energy-band diagram that illustrates the six different groups of photogenerated electrons out of the heavy-hole, light-hole, and split-off band to the Γ valley of the conduction band.

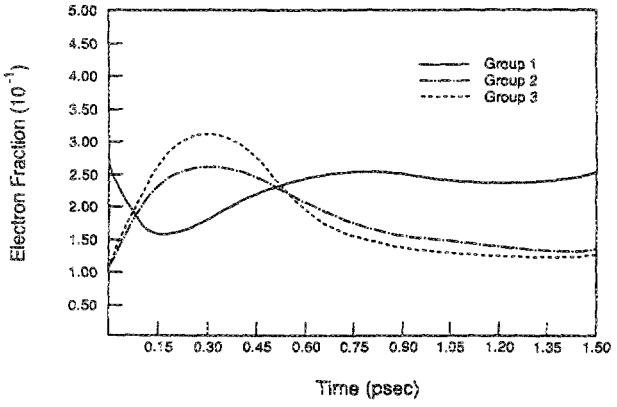

FIG. 10. The fractional population of electrons in the Γ valley vs time of groups 1, 2, and 3 shown in Fig. 9. The applied field is 20 kV/cm and the laser energy is 2.0 eV.

increase during the period of time in which they are being accelerated into the high-energy states and then decrease to a steady-state value as a result of intervalley scattering. The main point to be concluded from Figs. 10 and 11 is that electrons from groups 1, 2, and 3 constitute the majority of the Γ-valley electrons in the first few hundred femtoseconds. This interplay between field acceleration and intervalley scattering is very similar to that of the Jones–Rees effect[12] seen in Gunn devices.

The average velocity in the Γ valley of groups 1, 2, and 3, shown in Fig. 12, starts at a large negative value, becomes positive, and then overshoots before reaching a positive steady-state value. Since they constitute the majority of Γ-valley electrons, their negative velocity in the first few hundred femtoseconds will slow the initial rise of the drift velocity. The initial negative average value of the velocity of these electrons is determined by the wavelength and the band structure. It, therefore, is field independent. However, as the value of the applied field increases, the velocity will rise faster. This causes the bias-dependent shift to an earlier rise of the velocity with higher applied field as shown in Fig. 4. It is this portion of the electrons that produces an overall velocity overshoot.

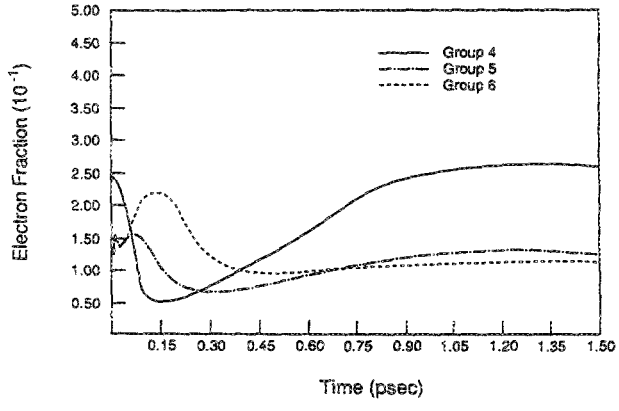

FIG. 11. The fractional population of electrons in the Γ valley vs time of groups 4, 5, and 6 shown in Fig. 9. The applied field is 20 kV/cm and the laser energy is 2.0 eV.

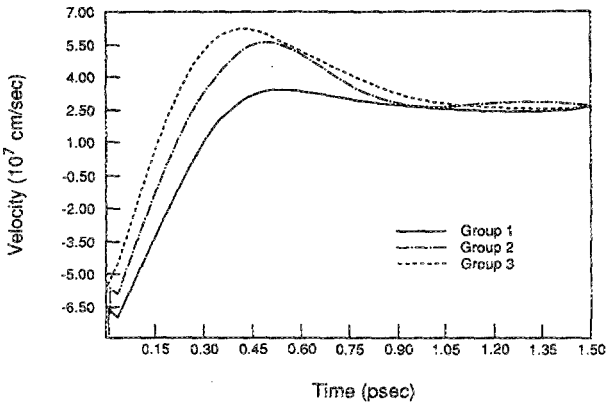

FIG. 12. Transient velocity for electron groups 1, 2, 3 for a 20-kV/cm field and laser energy of 2.0 eV.

It is easy to see why such a delay is not expected when one starts out with a thermal distribution. The initial energy is much lower than the threshold for intervalley transfer. It is, therefore, not possible to create a sizeable population of negative velocity electrons in the Γ valley. The Monte Carlo results of Fig. 4 confirm this. The velocity for the thermalized distribution rises sharply and shows an overshoot, while the one with the photogenerated carriers does not. Extending the same reasoning, it becomes evident that parameterized models of the transient photoconductive process,[35] will not show this effect. These models are based upon an *a priori* assumption of the form of the distribution function which is evaluated by taking the moments of the time-dependent Boltzmann equation. This procedure, in essence, leads to the masking of the true momentum distribution. For more realistic simulations using the analytic approaches, one needs to approximate the electron distribution function more accurately. This, in fact, is what Jones and Rees did in their work where they used an iterative solution of the Boltzmann equation in which the distribution function was constructed from an appropriately chosen basis set.

In summary, the Monte Carlo studies show that the nature of the transient response depends on both the wavelength of the excitation and the magnitude of the applied electric field (Table II). For wavelengths long enough that no electrons are generated into states lying near or above the energy threshold for intervalley scattering, a quite conventional velocity overshoot occurs. For shorter wavelengths new features appear as a result of a ballistic trapping of negative velocity electrons in the Γ valley. There will be a bias-dependent delay in the rise of the velocity associated with the time required to accelerate these negative velocity electrons into positive velocity states. If a velocity overshoot occurs it is because of a velocity overshoot of these ballistically selected Γ valley electrons. The minimum field required for the existence of a velocity overshoot becomes wavelength dependent and will be larger than is expected from a conventional velocity overshoot study. The exact value of this field cannot be predicted with more than 20% accuracy inside the parameter variation allowed by our present knowledge. Therefore, experimental determination of this value is needed and this type of experimental knowledge can then be used to more accurately constrain the parameter specification used in Monte Carlo studies.

TABLE II. Parameters for GaAs Monte Carlo program as given in Ref 7.

Parameter		Γ	L	X
Density (g/cm^3)	5.36			
Energy-band gap at 300 K (eV)	1.43			
High-frequency dielectric constant	10.92			
Static dielectric constant	12.9			
Velocity of sound (cm/s)	5.24×10^5			
Number of valleys		1	4	3
Effective mass ratio				
m_l		0.063	1.5	1.5
m_t		0.063	0.10	0.25
Nonparabolicity factor (eV^{-1})		0.69	0.64	0.55
Valley separation from Γ valley (eV)			0.33	0.52
Polar optic-phonon energy (eV)		0.035	0.0343	0.0343
Acoustic deformation potential (eV)		8.0	8.0	8.0
Coupling constant (10^8eV/cm)				
from Γ valley to			10	10
from L valley to		10	10	9
from X valley to		10	9	9
Intervalley phonon energy (eV)	0.026			
Heavy-hole band	0.70			
Light-hole band	0.082			
Split-off band	0.20			

IV. PHOTOCONDUCTIVITY EXPERIMENT

Here we describe a time-resolved photoconductivity experiment performed at the University of Rochester, Rochester, New York by Meyer *et al.*[36,37] This experiment represents a significant advance over earlier work.[1,2] All measurements were done using nominally undoped ($n = 5\times10^{15}$ cm^{-3}) high-mobility GaAs grown via MBE at Cornell University or metalorganic chemical vapor deposition (MOCVD) at SPIRE Corporation. Two micrometers of undoped material were grown on semi-insulating substrates, followed by a 500-Å layer of highly doped ($n^+ = 2\times10^{18}$ cm^{-3}) GaAs. Various test structures were patterned using lift-off photolithography. The evaporated NiAuGe contacts were furnace annealed, and in conjunction with the doped cap layer formed highly reproducible ohmic contacts, indicated by a quasi-linear dc I-V characteristic to fields as high as 10 kV/cm. A calibrated GaAs etch was used to remove the doped cap layer in the photoconductive gaps and between the transmission lines.

Two laser sources were used to excite and probe the

transient photoconductivity. For the first set of measurements a colliding pulse mode-locked (CPM) laser was utilized, which has a wavelength of 620 nm, a repetition rate of 100 MHz, a pulse width of 60 fs, and an average power of 5 mW per beam. In subsequent experiments a linear-cavity near-IR laser was used, which generated 300-fs pulses at 760 nm at a repetition rate of 100 MHz and an average power of 10 mW.

Measurement of the transient voltage waveforms was accomplished using reflection-mode electro-optic sampling.[38] In this embodiment, illustrated in Fig. 13, a thin plate of $LiTaO_3$ with a high-reflectivity coating on one surface is placed on top of the GaAs sample with the coating in contact with the GaAs. A small window was etched in the coating to allow for transmission of the excitation beam, which was focused symmetrically on the photoconductive gap. The probe beam was focused between the transmission lines a short distance from the gap. Fringing fields from the substrate extend into the electro-optic superstrate and are detected as a change in polarization of the probe beam. The probe beam is optically biased to assure that the polarization changes linearly with the electric field. A dc voltage was applied to the transmission line and the corresponding optical change was recorded to calibrate the measurement. An optical delay line changes the pump-probe delay, and the subsequent time-dependent signal is recorded using an rf mixer, lock-in amplifier, and signal averager. The overall experimental setup is shown in Fig. 14.

The temporal resolution of such an experiment is limited by four factors.[39] It can be written as a sum-of-squares convolution of these factors as

$$\tau_{\exp} = (2\tau_l^2 + \tau_o^2 + \tau_e^2 + \tau_i^2)^{1/2}, \qquad (1)$$

where τ_l is the laser pulsewidth, τ_o is the transit time of the optical probe pulse across the electric field lines, τ_e is the electrical transit time across the optical probe beamwaist, and τ_i is the intrinsic electro-optic response time. τ_o is determined by the transmission line geometry and τ_e is determined by the optical beam size. For the coplanar geometry used here, τ_o is governed by the penetration depth of the field into the substrate. Assuming a τ_i of 50 fs (Ref. 40) for lithium tantalate, a probe beam spot size of 5 μm, stripline dimensions of 10 μm, and a laser pulse width of 50 fs, a practical resolution limit of 150 fs is obtained. This should be quite adequate for the practical determination of a velocity overshoot.

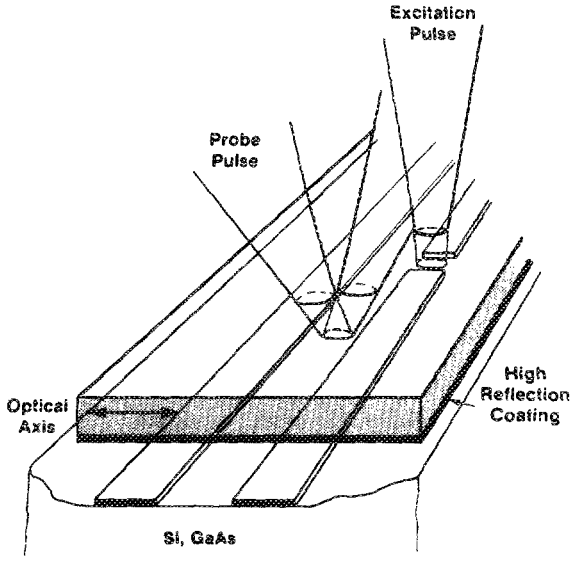

FIG. 13. Reflection mode electro-optic sampling geometry.

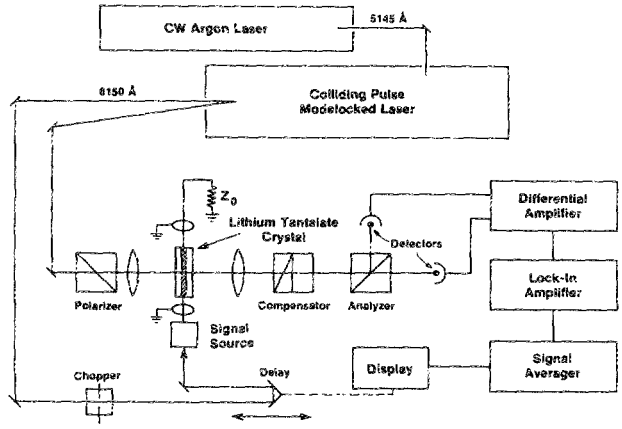

FIG. 14. The overall experimental setup for the photoconductivity experiment.

Several other points of interest should be noted. First, the exact delay between the pump and probe pulses is not known. Therefore, one should be careful not to assume that the time origin shown on the following experimental data actually corresponds to the temporal incidence of the pump pulse onto the gap. Second, the resolution figure quoted above limits our ability to resolve two separate features on a single experimental trace. There is another important resolution, however. A very useful experimental procedure is to first collect a trace for one bias, change only the bias setting, and repeat the experiment without altering the laser system in any way. The critical question then is how accurately can we measure the temporal shift in a single feature as a function of bias? The resolution just described does not limit this. The bias delay resolution instead is limited primarily by our ability to accurately calibrate the extra path delay added in the experiment and by τ_l. For the short wavelength case presented here bias induced temporal shifts of 60 fs can be resolved. This mode of experimentation therefore allows us to accurately search for the bias-dependent delays discussed in the Monte Carlo section.

One last comment should be made concerning this experimental technique. The electro-optic sampling technique is very sensitive and quite capable of measuring submillivolt changes in line voltage. This allows for the possible use of this technique in low excitation experiments where carrier-carrier scattering and hot phonon effects are unimportant.

The particular sample geometry consisted of 50-μm-wide coplanar strip lines separated by a 50-μm spacing, and the photoconductive gap length was also 10 μm. The pump and probe beams were each separately focused to approxi-

mately 10 μm, and the probe beam was positioned 20 μm downstream from the photoconductive gap. Results obtained with 620-nm excitation are shown in Fig. 15, plotted as the transient voltage normalized to the gap bias voltage. The measured transient voltage is only 0.01% of the applied bias voltage and therefore the associated displacement current is much smaller than the particle current. Two features are clearly present in the data: a significant photocurrent overshoot that occurs at high biases but not at moderate or low biases, and a much faster rise time of the photocurrent for high biases.

For the reasons described earlier, it was desirable to repeat the experiment at a longer excitation wavelength. Photocurrent transients obtained with 760-nm excitation are shown Fig. 16. Once again, a photocurrent overshoot is observed at high bias and not at low bias. Unfortunately a larger overshoot was not observed because the 300-fs pulsewidth of the pump and probe in this case limited the temporal resolution of the measurements. No bias-dependent delay was observed here. While this is consistent with the Monte Carlo studies, the poorer temporal resolution in this case may have obscured the observation of such a delay.

In order to more fully understand this experiment, we extended the basic Auston model[25] of the photoconductive gap for our simulations of the photoconductivity experiment. The original Auston model for the photoconductive gap consisted of a capacitor in parallel with a linear conductance. In that model, the characteristic impedance of the transmission lines had been taken to be frequency independent. Reflection effects at the transmission line were neglected because the transient switching time of interest was much less than the transit time through the transmission lines.

In the new model[5] illustrated in Fig. 17, the conductance is replaced by a photoconductive element, and the characteristic impedance of the transmission lines is taken to be frequency dependent. The Monte Carlo model for electron transport in GaAs described in Sec. III, is used to simulate the photoconductive element. The inclusion of the Monte Carlo correctly builds in all the nonlinearities associated with transient transport in the photoconductive

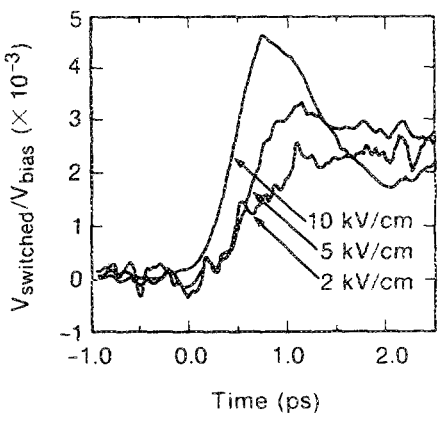

FIG. 15. Transient voltage waveform generated by the photoconductive switch normalized to the applied dc bias for excitation wavelength of 620 nm.

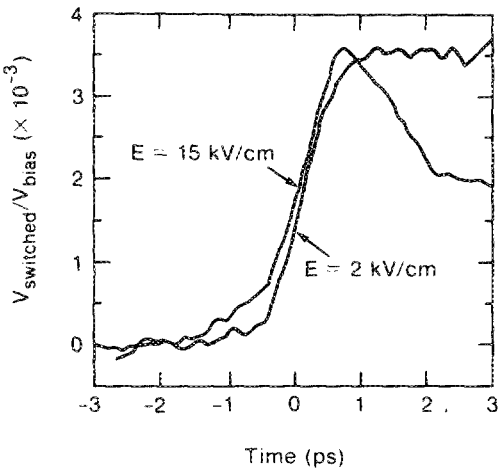

FIG. 16. Transient photoconductivity results for excitation wavelength of 760 nm.

switch and allows us to obtain the appropriate photocurrent contribution. However, a simple spatially constant field was assumed and therefore space-charge effects will not appear here. The Monte Carlo routine is embedded in a circuit simulation program in order to obtain a complete model and calculate the output voltage. The circuit program uses the impulse-response method of the time-domain analysis.[41] Prior to photoexcitation, the voltage across the gap is

$$V_G(0) = V_{\text{bias}} - I_{\text{Dark}} R_L, \tag{2}$$

where I_{dark} is measured experimentally. When the laser source is turned on, the input and ouput voltages are given as the sum of a dc component and a time-varying component:

$$V_{\text{in}}(t) = V_{\text{bias}} - V_w(t), \tag{3}$$

$$V_{\text{out}}(t) = I_{\text{dark}} R_L + V_w(t). \tag{4}$$

As is obvious from Eq. (4), the time-varying part need not be small compared to the initial steady-state component. The time-varying total current $I_{\text{total}}(t)$ is given by the following expression:

$$I_{\text{tot}}(t) = C_{\text{gap}} \frac{d}{dt}[V_{\text{in}}(t) - V_{\text{out}}(t)] + I_{\text{ph}}\{V_{\text{in}}(t) - V_{\text{out}}(t)\}. \tag{5}$$

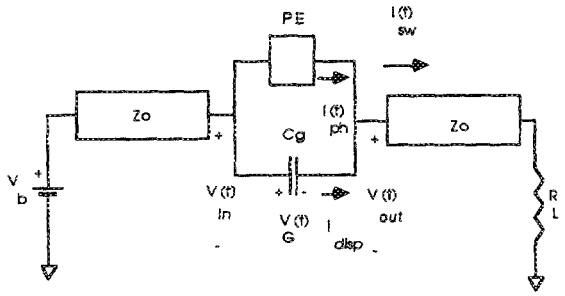

FIG. 17. The equivalent circuit used for the switch analysis.

In the above, the photocurrent I_{ph} is a function of the voltage across the gap, and thus behaves as a voltage-controlled current source. This particle photocurrent corresponding to the voltage drop across the gap can be obtained using the Monte Carlo program. It is based on the following equation:

$$I_{ph}\{V_{in}(t) - V_{out}(t)\} = qnAV_d, \tag{6}$$

where n was the electron concentration, A is the area across which the current flows, and V_d is the ensemble averaged velocity during the appropriate time step.

The left-hand side of Eq. (5) is determined by the characteristic of the transmission line and is evaluated through the convolution integral

$$I_{total}(t) = \int_0^t V_w(\tau) Y_0(t-\tau) d\tau + I_{dark}. \tag{7}$$

In the above equation, $Y_0(t)$ is the impulse-response (or inverse transfrom of the characteristic admittance) of the transmission line. Implicit in the above equation is the assumption that the signal flow is unidirectional, and hence the line impedance is not modified by the load termination. This is valid within the time scales of interest here as the transmission line lengths were in the millimeter range. We use the transmission line model of Whitaker *et al.*[42] which has been used in modeling dispersion in similar experiments. This transmission model, although somewhat empirical, satisfies causality with the function $[Z_0(\omega) - 1]$ having poles only in the lower half-plane. This satisfies the condition that $G(\tau)$ defined as

$$G(\tau) = \left(\frac{1}{2\pi}\right) \int_{\infty}^{\infty} [Z_0(\omega) - 1] \exp(-i\omega\tau) d\omega, \tag{8}$$

is zero for all τ less than zero. Comparing Eqs. (5) and (7), we get an equation for the unknown $V_w(t)$:

$$C_{gap} \frac{d}{dt}[V_{in}(t) - V_{out}(t)] + I_{ph}[V_{in}(t) - V_{out}(t)] = \int_t^0 V_w(\tau) Y_0(t-\tau) d\tau + I_{dark}. \tag{9}$$

The above equation was solved numerically using the classical Runge–Kutta method with forward differencing.

The geometry of the structure simulated is the following: The gap length is 10 μm and the transmission linewidth is 50 μm. The separation between the two transmission lines is 50 μm and the probe beam is 20 μm down the line from the gap. The laser power is the 5 mW per beam for excitation wavelength of 620 nm. The carrier concentration density used is 5×10^{15} cm^{-3}. The capacitance value for this case is 1 fF.

The results obtained from this simulation for the output voltage using a initial bias of 10 and 20 V and an excitation wavelength of 620 nm are shown in Fig. 18. The corresponding electron drift velocity curves are shown in Fig. 19. For both bias cases, we notice that the shape of the velocity is translated into the shape of the output voltage.

We also considered the problem from a different perspective and extracted the photocurrent from the experimentally measured voltage. This was done by removing the Monte Carlo model from the circuit simulation and calculating the photocurrent using the output voltage as an input parameter. The magnitude of the extracted photocurrent was less than that predicted by the Monte Carlo model using Eq. (1). We believe this descrepancy arises from the assumption of a spatially uniform field across the gap. In the n^+-i-n^+ structure used, the field is nonuniform and takes on positive and negative values depending on the position. Electrons in some regions of the gap will possess negative velocity with respect to the direction of the field and this will reduce the value of the total drift velocity and the photocurrent. More exact modeling requires the inclusion of a Poisson solver in the Monte Carlo to find the field with respect to position is necessary and will yield closer results to those seen experimentally. A more fruitful approach is the development of a new experiment using a vertically oriented p-i-n structure where a uniform field can be more safely assumed, as done in microwave time-of-flight experiments.[20,21]

In summary, existing experiments clearly show that

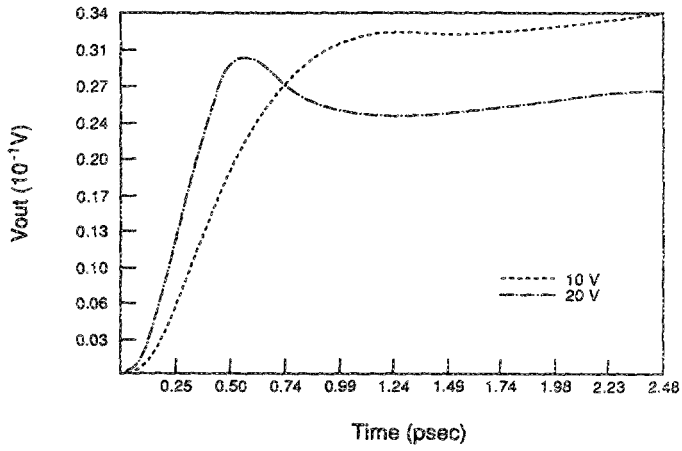

FIG. 18. The transient output voltage normalized to the dc bias obtained from circuit simulation. The pulse energy is 2.0 eV (620 nm) and the dc bias are 10 and 20 V.

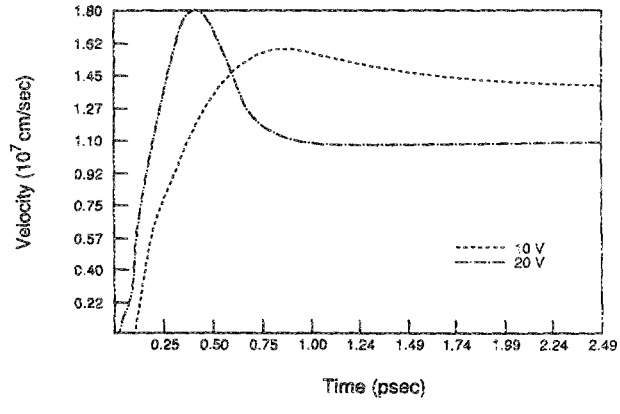

FIG. 19. The transient electron velocity corresponding to Fig. 17 for bias of 10 and 20 V and pulse energy of 2.0 eV.

electro-optic sampling has both the temporal resolution and sensitivity to measure transients excited by transient transport in the photoconductive switch. Circuit analysis clearly shows that a transient transport produced photocurrent transient can create similar transmission line voltage transients. Monte Carlo studies show that a carefully conducted version of such experiments may be able to more completely restrict the value of the Γ-L coupling coefficient. However, a carefully conducted experiment requires the use of low photoexcitation levels in structures specifically designed to produce quasi-one-dimensional electric fields.

ACKNOWLEDGMENT

This work was supported in part by the Air Force Office of Scientific Research.

[1]R. B. Hammond, Physica B **134**, 475 (1985).
[2]G. Mourou, K. Meyer, J. Whitaker, M. Pessot, R. Grondin, and C. Caruso, in *Picosecond Electronics and Optoelectronics II. Vol. 24 in Springer Series in Electronics and Photonics* (Springer, Berlin, 1987), p. 40.
[3]M.C. Nuss, D. H. Auston, and F. Capasso, Phys. Rev. Lett. **58**, 2355 (1987).
[4]M. Osman and H. Grubin, Solid-State Electron. **31**, 471 (1988).
[5]R. O. Grondin and M. J. Kann, Solid-State Electron. **31**, 567 (1988).
[6]A. Evan Iverson, G. M. Wysin, D. L. Smith, and A. Redondo, Appl. Phys. Lett. **52**, 2148 (1988).
[7]G. M. Wysin, D. L. Smith, and A. Redondo (unpublished).
[8]J. G. Ruch, IEEE Trans. Electron Devices **ED-19**, 652 (1972).
[9]M. A. Osman and D. K. Ferry, J. Appl. Phys. **61**, 5330 (1987).
[10]H. D. Rees, IBM J. Res. Dev. **13**, 537 (1969).
[11]R. O. Grondin, P. A. Blakey, and J. R. East, IEEE Electron. Devices **31**, 21 (1984).
[12]D. Jones and H. D. Rees, J. Phys. C **6**, 1781 (1973).
[13]D. Jones and H. D. Rees, Electron. Lett. **8**, 363 (1972).
[14]G. Bernstein and D. K. Ferry, Superlattices and Microstructures **2**, 373 (1986).
[15]M. Heiblum, I. M. Anderson, and C. M. Knoedler, Appl. Phys. Lett. **49**, 207 (1986)
[16]J. R. Hayes, A. F. J. Levi, and W. Wiegmann, Electron. Lett. **20**, 851 (1984).
[17]C. V. Shank, R. L. Fork, B. I. Greene, F. K. Reinhart, and R. A. Logan, Appl. Phys. Lett. **38**, 104 (1981).
[18]S. Ramo, Proc. IRE **27**, 584 (1939).
[19]W. Shockley, J. Appl. Phys. **9**, 635 (1981).
[20]P. M. Smith, M. Inoue, and J. Frey, Appl. Phys. Lett. **37**, 797 (1980).
[21]T. H. Windhorn, T. J. Roth, L. M. Zinkiewicz, O. L. Gaddy, and G. E. Stillman, Appl. Phys. Lett. **40**, 513 (1982).
[22]L. V. Keldysh, Sov. Phys. JETP **7**, 778 (1958).
[23]W. Potz, P. Kocevar, Phys. Rev. B **28**, 7040 (1983).
[24]J. Shah, B. Deveaud, T. C. Damen, W. T. Tsang, A. C. Gossard, and P. Lugli, Phys. Rev. Lett. **59**, 2222 (1987).
[25]D. H. Auston, IEEE J. Quantum Electron. **QE-19**, 639 (1983).
[26]J. A. Valdmanis, G. A. Mourou, C. W. Gabel, IEEE J. Quantum Electron. **QE-19**, 664, (1983).
[27]S. Teitel and J. W. Wilkins, J. Appl. Phys. **53**, 5006 (1982).
[28]S. J. Allen C. L. Allyn, H. M. Cox, F. DeRosa, and G. E. Mahoney, Appl. Phys. Lett. **42**, 96 (1983).
[29]E. O. Kane, J. Phys. Chem. Solids **1**, 249 (1957).
[30]M. A. Osman, D. K. Ferri, Phys. Rev. B **36**, 6018 (1987).
[31]M. Rieger, P. Kocevar, P. Bordone, P. Lugli, and L. Reggiani, Solid-State Electron. **31**, 687 (1988).
[32]D. E. Aspnes, Phys. Rev. B **14**, 5331 (1976).
[33]K. Brenan, and K. Hess. Phys. Rev. B **29**, 5581 (1984).
[34]A. J. Taylor, D. J. Erskine, and C. L. Tang, J. Opt. Am. B **2**, 663 (1985).
[35]V. N. Freire, A. R. Vasconcellos, and R. Luzzi, Solid State Commun. **66**, 683 (1988).
[36]K. E. Meyer, M. Pessot, G. Mourou, R. O. Grondin, and S. N. Chamoun, Appl. Phys. Lett. **53**, 2254 (1988).
[37]K. E. Meyer, Ph. D. dissertation, University of Rochester, 1988.
[38]K. Meyer, and G. Mourou, in *Picosecond Electronics and Optoelectronics*, edited by G. Mourou, D. Bloom, and C. Lee (Springer, Berlin, 1985), Vol. 21.
[39]J. A. Valdmanis, Ph.D. dissertation, University of Rochester, 1983.
[40]D. H. Auston, K. P. Cheung, J. A. Valdmanis, and D. A. Kleinman, Phys. Rev. Lett. **53**, 1555 (1984).
[41]E. N. Arnold, M. S. thesis, Arizona State University, 1988.
[42]J. F. Whitaker, R. Sobolewski, D. Dykaar, T. Hsiang, and G. Mourou, IEEE Trans. Microwave Theory Tech. **MTT-36**, 277 (1988).